Tellus (1991), *43A*, 235–245

A three-layer model of ocean fronts

By HELEN M. WALLACE* and ANDREW J. WILLMOTT, *Department of Mathematics, University of Exeter, North Park Road, Exeter, England, EX4 4QE*

(Manuscript received 1 June 1990; in final form 13 November 1990)

ABSTRACT

A three-layer, steady-state, wind-driven model of the thermocline is used to investigate the structure of ocean density-fronts. Analytical expressions are derived for the shape of the upper-layer outcropping line in terms of the applied wind stress. It is found that the presence of interfacial friction is crucial in determining the outcropping line, and that real wind stress data can produce very different outcrop curves to commonly used analytical winds. For a simplified, inviscid model, the layer depths and streamfunctions are also calculated. It is shown that stronger flow occurs in the subducted second layer than in the directly driven surface layer.

1. Introduction

The importance of the problem of the ventilated thermocline in understanding the vertical structure of oceanic circulation has been emphasized by Luyten et al. (1983), who considered a layered model in which the upper layers outcrop along prescribed lines (latitude circles are chosen to make the problem analytically tractible). When outcropping occurs, the lower layers are thus exposed to Ekman pumping, and the motion of each can be traced into a region where it is shielded from direct forcing, since columns of fluid conserve potential vorticity once they are subducted. Fig. 1 illustrates the concept of "outcropping" in a layered ocean. A very different circulation pattern emerges to that given by a model in which the lower layers are never exposed to direct forcing and consequently remain motionless except within contours of potential vorticity (Rhines and Young, 1981). However the model of Luyten et al. (1983) and subsequent extensions, which include both buoyancy and wind driven circulation (Luyten and Stommel, 1986; Pedlosky, 1986) assume prescribed (constant latitude) outcropping lines for each layer. In this paper an attempt is made to determine the outcropping lines that can exist in a three-layer wind-driven model.

* Present address: Hydraulics Research Ltd., Wallingford, Oxon, OX10 8BA, UK

An earlier attempt to determine the outcropping lines was made by Pedlosky et al. (1984), who couple the model of Luyten et al. (1983) to a simple model of the oceanic mixed layer. The outcrop position is then determined by a combination of advection and surface heating. However, surface heating must be limited to the transition zone between two layers of different density, i.e., occur only at the outcrop lines, in order for fluid to pass across the outcrop lines and immediately change density. In contrast, Parsons (1969) considered outcropping in a two-layer model, consisting of an active surface layer above an infinitely deep quiescent layer. When the amount of fluid in the upper layer is reduced to a critical level the layer outcrops along a surfacing line which must be a streamline (since the layers are assumed immiscible). If the outcrop is not a streamline of the interior Sverdrup solution a boundary layer must exist along it, and its shape is determined by the boundary layer dynamics. In this type of model (which has been extended by Kamenkovich and Reznik (1972), Veronis (1973) and Huang and Flierl (1987)), the mixed layer is included within the depth integrated flow in the upper layer and there is no surface heating.

The main limitation of the two layer model is that it is not possible to study the flow of the lower, ventilated layer, since this is always assumed infinitely deep and motionless, even when the upper layer has outcropped, exposing it to direct

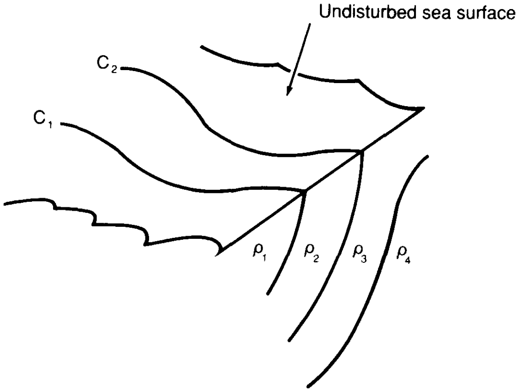

Fig. 1. Schematic representation of a layered ocean in which the layers of constant density ρ_1 and ρ_2 outcrop along the curves C_1 and C_2 respectively. In Luyten et al. (1983), the outcrop lines are assumed to coincide with latitude circles, for analytical convenience.

forcing. In this paper, the two approaches (of Luyten et al., 1983 and Parsons, 1969) are combined. A three-layer model of the ocean circulation is developed and possible outcropping lines are calculated, for both idealized (zonal) and real wind stress (seasonal data, from Hellerman (1967, 1968)). For a simplified, inviscid model, the layer depths are calculated by integration of a first-order partial differential equation along characteristics (similar to the method of Luyten and Stommel (1986)), and the flow in the lower layer is calculated using the potential vorticity conservation method of Luyten et al. (1983). However, it is shown that the presence of interfacial friction is crucial in determining the outcrop lines.

2. Model equations

Consider a steady-state model consisting of two active fluid layers above an infinitely deep, quiescent layer of constant density, ρ_0, as illustrated in Fig. 2a. The model is an extension of the reduced gravity formulation of Niiler et al. (1971). The upper two active layers have densities ρ_1 and ρ_2, which in general may be functions of the latitude and longitude, and the circulation is driven by a surface wind stress τ_0, acting as a body force on the upper layer, and by a surface heating function. The vertically integrated momentum equations are:

$$h_1 v_1 = (\tfrac{1}{2}f)(h_1^2 b_1)_x + (h_1/f)(b_2 h_2)_x - \tau_0^x/f + (k_1/f)(u_1 - u_2), \qquad (1)$$

$$h_1 u_1 = -(\tfrac{1}{2}f)(h_1^2 b_1)_y - (h_1/f)(b_2 h_2)_y + \tau_0^y/f - (k_1/f)(v_1 - v_2), \qquad (2)$$

$$h_2 v_2 = (\tfrac{1}{2}f)(h_2^2 b_2)_x + (h_2 b_2/f)\, h_{1x} - (k_1/f)(u_1 - u_2), \qquad (3)$$

$$h_2 u_2 = -(\tfrac{1}{2}f)(h_2^2 b_2)_y - (h_2 b_2/f)\, h_{1y} + (k_1/f)(v_1 - v_2), \qquad (4)$$

in which the velocities in each layer are $\boldsymbol{v}_i = (u_i, v_i)$ where $i = 1, 2$ (the subscript 1 referring to the upper layer and 2 to the middle layer), h_i and b_i are the instantaneous thickness and the buoyancy of each layer respectively, f is the Coriolis parameter, k_1 is the constant coefficient of friction between the two active layers and x, y and z are the eastward, northward and vertical coordinates, respectively, on a local beta-plane. The buoyancies are defined by

$$b_1 = (\rho_0 - \rho_1)\, g/\rho_0,$$

$$b_2 = (\rho_0 - \rho_2)\, g/\rho_0,$$

where g is the acceleration due to gravity.

It is assumed: (i) the layers are immiscible; (ii) the lowest layer is infinitely deep and motionless; (iii) the effect of friction between the lower two layers is negligible and that between the two active layers is proportional to the difference in their velocities; (iv) the flow can be represented by the vertically averaged velocities; (v) the Boussinesq approximation holds.

If interfacial friction is also introduced between the lower two layers, the problem becomes mathematically intractable. However, in this study the goal is to determine the outcrop curve, along which the depth of the upper active layer vanishes (see Fig. 1). The inclusion of interfacial friction between the two active layers is likely to be more crucial in determining the shape of this outcrop than the equivalent friction acting between the lower two layers. The conservation of mass and heat equations in the active layers are:

$$(h_1 u_1)_x + (h_1 v_1)_y = 0, \tag{5}$$

$$(h_2 u_2)_x + (h_2 v_2)_y = 0, \tag{6}$$

$$h_1 u_1 b_{1x} + h_1 v_1 b_{1y} = \alpha g(Q_0 - Q), \tag{7}$$

$$h_2 u_2 b_{2x} + h_2 v_2 b_{2y} = \alpha g Q, \tag{8}$$

where Q_0 and Q are the rates at which the ocean surface and the second layer are heated respectively, and α is the thermometric expansion coefficient of sea water.

Substitution of the individual layer transports (1) to (4) into the total continuity equation (namely, the sum of (5) and (6)) gives the Sverdrup relation:

$$(\beta/2f^2)(h_1{}^2 b_1 + h_2{}^2 b_2 + 2h_1 h_2 b_2)_x = \boldsymbol{k} \cdot \nabla \wedge (\tau_0/f), \tag{9}$$

This may be integrated to give

$$h_1{}^2 b_1 + h_2{}^2 b_2 + 2h_1 h_2 b_2 = K(x, y) + F(y), \tag{10}$$

where

$$K = (2f^2/\beta) \int_0^x \boldsymbol{k} \cdot \nabla \wedge (\tau_0/f)\, \mathrm{d}x, \tag{11}$$

$$F(y) = (h_1{}^2 b_1 + h_2{}^2 b_2 + 2h_1 h_2 b_2)_{x=0}, \tag{12}$$

and $x = 0$ is the eastern boundary.

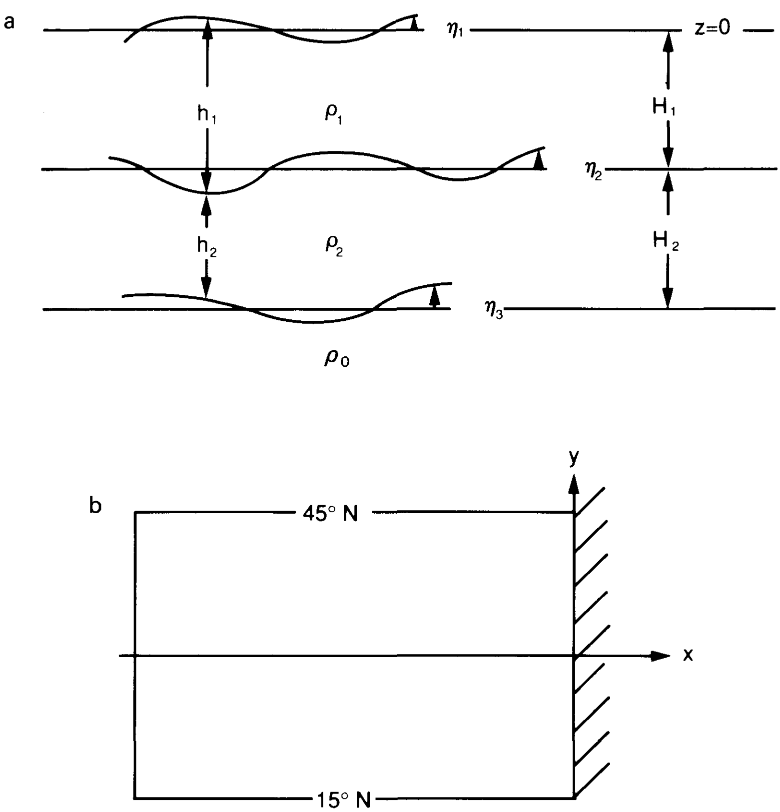

Fig. 2. Geometry of the Model. (a) Diagram of the three layers. (b) Plan view of the domain, representative of the North Atlantic or North Pacific subtropical gyre.

Eq. (10) holds for a single active layer, when $h_1 = 0$, and may be solved for h_2 if h_1 is known and $F(y)$ and $\boldsymbol{\tau}_0$ are prescribed.

3. Boundary conditions

The domain of interest is illustrated in Fig. 2b. A region between the latitudes 15° N and 45° N is considered, representing the subtropical gyre. A closed eastern boundary exists at $x = 0$, but no attempt is made to model the western boundary layer dynamics. The origin of the coordinate system is at 30° N on the eastern boundary.

Requiring no flow through the eastern boundary gives

$$F = 2\int_{y_0}^{y} (\tau_0{}^y)_{x=0}\,\mathrm{d}y + F_0, \tag{13}$$

where F_0 is a constant given by

$$F_0 = (h_1{}^2 b_1 + h_2{}^2 b_2 + 2h_1 h_2 b_2)_{(x=0,\, y=y_0)}. \tag{14}$$

The point $(0, y_0)$ is chosen such that the upper layer depth is zero, so that

$$F_0 = h_0{}^2 b_2, \tag{15}$$

where $h_2 = h_0$ at $(0, y_0)$.

In addition to (13), it is required that the flow into the eastern boundary in the lower layer is zero, so that the upper layer flow normal to the eastern boundary is automatically zero. (Provided the interface between layers 1 and 2 is material). That is

$$0 = (h_2{}^2 b_2)_y + 2h_2 b_2 h_{1y} - 2k_1(v_1 - v_2) \quad \text{on} \quad x = 0. \tag{16}$$

In the special case where the coefficient of friction is zero and b_2 is constant (a purely wind driven model), (16) implies

$$h_2 = 0 \quad \text{or} \quad h_1 + h_2 = c_0 \quad \text{on} \quad x = 0, \tag{17}$$

where c_0 is a constant.

4. Frictionless, wind-driven model equations

Consider a purely wind-driven, frictionless model, in which $k_1 = 0$, $Q_0 \equiv 0 \equiv Q$ and the buoyancies b_1 and b_2 are constants. In this simplified case, a single partial differential equation for h_1 can be obtained by substituting (3) and (4) (with $k_1 = 0$) into the lower layer continuity equation and eliminating h_2 using (10). The resulting equation is

$$\{2\beta(h_1 b_2 - C)\, h_1(b_2 - b_1) + f b_2 (K + F)_y\}\, h_{1x} - f b_2 K_x h_{1y} = \beta K_x(-h_1 b_2 + C), \tag{18}$$

where

$$C = [b_2\{h_1{}^2(b_2 - b_1) + K + F\}]^{1/2}.$$

Eq. (18) is a quasilinear PDE, which may be solved for h_1 using the method of characteristics. The lower layer depth h_2 can then be found from (10). In addition, it is convenient to define streamfunctions to satisfy (5) and (6) identically:

$$h_1 u_1 = -\Psi_{1y} \qquad h_1 v_1 = \Psi_{1x}$$
$$h_2 u_2 = -\Psi_{2y} \qquad h_2 v_2 = -\Psi_{2x} \tag{19}$$

and the total streamfunction,

$$\Psi = \Psi_1 + \Psi_2. \tag{20}$$

In terms of Ψ, the Sverdrup relation may now be written as

$$\Psi = (1/\beta)\int_0^x \boldsymbol{k}\cdot\nabla \wedge \boldsymbol{\tau}_0\,\mathrm{d}x + \Psi_0(y), \tag{21}$$

so that streamlines of the total flow can easily be calculated. To satisfy the condition of no flow through the eastern boundary, choose (without loss of generality)

$$\Psi_0 = 0. \tag{22}$$

Cross-differentiation of (3) and (4), and the use of the lower layer continuity equation, leads to

$$u_2(f/h_2)_x + v_2(f/h_2)_y = 0, \tag{23}$$

which states that lines of constant potential vorticity, $q = f/h_2$, are streamlines in the lower layer. Following Luyten et al. (1983), use may be made of this result to trace streamlines from a single active layer region (where $h_1 = 0$) to a region of two active layers, where the subducted layer is no longer directly forced.

5. Outcropping equations

Now consider the conditions under which the second layer may outcrop, so that the upper layer depth becomes zero along a line. For simplicity restrict the consideration of outcrops to those which intersect or asymptote to the eastern boundary and are streamlines of the interior flow, so that a boundary layer along the outcrop is not required.

The outcrop line, $y = y_1(x)$, is given by

$$h_{1x}\,\mathrm{d}x + h_{1y}\,\mathrm{d}y = 0 \quad \text{on} \quad y = y_1(x), \tag{24}$$

which, using the upper layer continuity equation (5), leads to

$$\mathrm{d}y_1/\mathrm{d}x = -h_{1x}/h_{1y} = v_1/u_1. \tag{25}$$

Eq. (25) is also derived by Huang and Flierl (1987) for the "super-critical" state of a two-layer model (in which the lower layer outcrops in the south-eastern corner of the basin and has a free eastern boundary where the streamfunction is zero). This equation is a direct result of allowing no flow between the different density layers.

6. The frictionless model ($k_1 = 0$)

Consider the frictionless ($k_1 = 0$), purely wind-driven model. As $h_1 \to 0$, the momentum equations give

$$\left.\begin{aligned} \tau_0{}^x &= 0 \\ \tau_0{}^y &= 0 \end{aligned}\right\} \quad \text{on} \quad y_1(x), \tag{26}$$

if u_1 and v_1 remain finite. Alternatively, if the transport components $h_1 u_1$ and $h_1 v_2$ remain finite but the velocities do not,

$$\left.\begin{aligned} h_1 v_1 &\to -\tau_0{}^x/f \\ h_1 u_1 &\to \tau_0{}^y/f \end{aligned}\right\} \quad \text{as} \quad h_1 \to 0,$$

and (25) becomes

$$\mathrm{d}y_1/\mathrm{d}x = -\tau_0{}^x/\tau_0{}^y. \tag{27}$$

This states that the Ekman transport is always tangential to the outcrop line, a result of the requirement that there is no flow between the layers. Huang and Flierl (1987) also derive this result (for the special case when the upper-layer streamfunction is zero), but for a two layer model in which the deep motionless lower layer must become exposed to the applied windstress at outcropping. In addition, their model includes friction (which has been omitted in this section) with the result that (27) only holds when the friction parameter is small compared to the upper layer depth. Obviously, this requirement is violated near the outcrop line as the upper layer depth tends to zero, so the validity of (27) in a model with non-zero friction is questionable (see Section 7).

Note that (27) holds even if the layer densities are not constant and surface heating is allowed. Pedlosky et al. (1984) obtained outcrops which depend on surface heating only by allowing flux across the interfaces between the layers and a heating function which was concentrated at the outcrop line, with a non-zero integral across it. Here, no flux is allowed between the layers and, consequently, the heating function is assumed continuous everywhere.

Now consider an applied idealized zonal wind-stress, given by

$$\tau_0{}^x = \tau_0 \sin(\pi y/\ell), \qquad \tau_0{}^y = 0, \tag{28}$$

where τ_0 is the maximum wind-stress magnitude and ℓ is the meridional length scale of the subtropical gyre. Inspection of (26) and (27) shows that the only outcrop to meet the eastern boundary is at $y = 0$.

The eastern boundary conditions for the frictionless model with zonal wind-stress give

$$h_1 = 0, \qquad h_2 = 0, \qquad \text{on} \quad x = 0,$$

so that the eastern boundary is also an outcrop for the upper layer (which is not inconsistent with (27)). Inspection of (18) shows that the eastern boundary is also a characteristic of this equation, which must therefore be integrated away from the known outcrop rather than the boundary.

Fig. 3 shows the layer depths for the frictionless model with zonal winds and an outcrop on the zero wind stress line $y = 0$. Not surprisingly the gradient of the lower layer depth is discontinuous at the outcrop line, where the three layer region begins, and the upper layer depth is largest in the south-west corner of the region, furthest from the eastern boundary and the outcrop line (where $h_1 = 0$). The results are similar to those of Luyten and Stommel (1986), who also integrate a PDE for h_1 along characteristics, but allow an interfacial flux not included here. It should be remembered that the circulation has not been closed by a western boundary current so the picture is not complete.

Fig. 4a shows the total Sverdrup streamfunction, calculated from (21) with the expected anticyclonic subtropical gyre. To the south of the outcrop, the lower layer streamfunction is calculated by tracing lines of constant potential vorticity into the subducted layer, using their known values on the outcrop. It is found that the stronger flow is in the lower layer, while the upper layer flow is cyclonic and weak (see Fig. 4b and 4c). This clearly illustrates the advantage of the three-layer model, since two-layer models (such as that of Huang and Flierl, 1987) assume the lower layer to be quiescent.

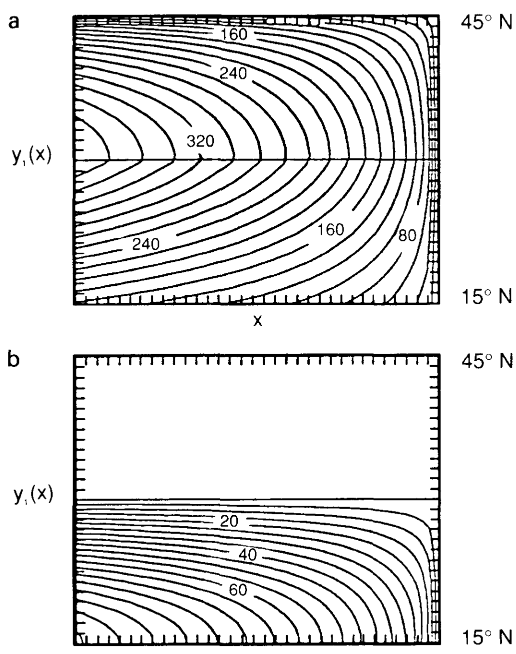

Fig. 3. The layer depths (in metres) for the frictionless model with zonal winds with $\tau_0 = 0.1\ \mathrm{Nm}^{-2}/\rho_0$. The buoyancies are $b_1 = 0.02\ \mathrm{ms}^{-2}$, $b_2 = 0.014\ \mathrm{ms}^{-2}$. (a) The lower layer depth, h_2; (b) the upper layer depth, h_1.

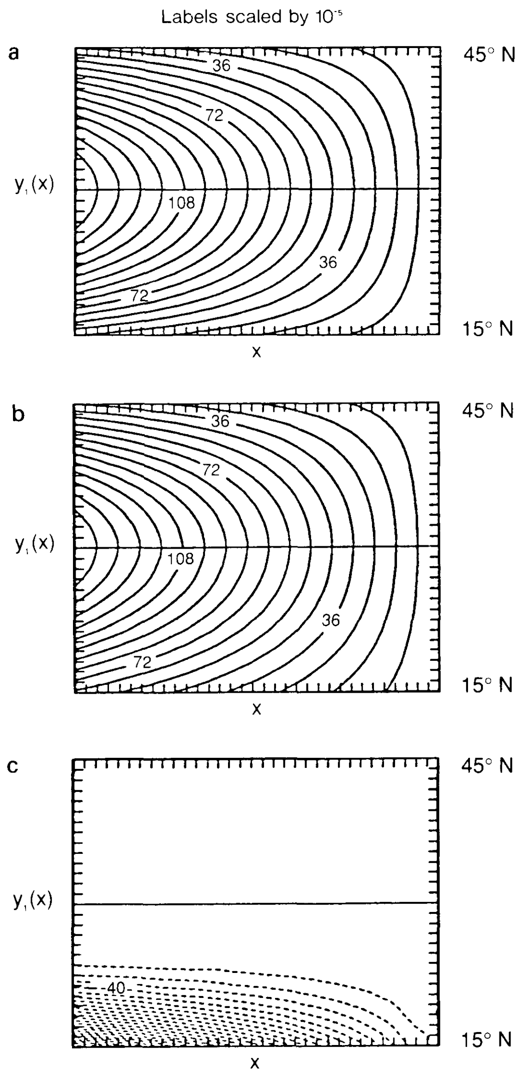

Fig. 4. The streamfunction ($\mathrm{m}^2\,\mathrm{s}^{-1}$) for the frictionless model with zonal winds with $\tau_0 = 0.1\ \mathrm{Nm}^{-2}/\rho_0$. The buoyancies are $b_1 = 0.02\ \mathrm{ms}^{-2}$, $b_2 = 0.014\ \mathrm{ms}^{-2}$. (a) The total streamfunction, Ψ; (b) the lower layer streamfunction, Ψ_2; (c) the upper layer streamfunction, Ψ_1.

Now consider a realistic applied wind stress. In this case the outcrop must satisfy (27) (since there is, in general, no line on which $\tau^y = \tau^x = 0$). As a result of the condition of no flow into the eastern boundary, as given by (17), the outcrop must asymptote to the boundary such that

$$\tau_0{}^y = 0 \qquad \text{at} \quad (0, y).$$

This is necessary because the flow along the outcrop is no longer zero.

Fig. 5 and 6 show the streamfunction and layer depths using real (seasonally averaged) wind stress data for spring in the North Pacific (Hellerman, 1967, 1968). The outcrop shape is markedly different to that predicted by the commonly used idealised winds, suggesting that the effects of a non-zero north-south wind component, in particular near the coast, are important in modelling ocean density fronts. However, the wind stress field is such that the outcrop line turns southwards until it reaches a region where $\tau_0{}^x$ and $\tau_0{}^y$ are both small. It remains near this region thereafter, so that the front then closely follows the line of Ekman convergence, as observed by Roden (1975).

The layer depth and streamfunction patterns are similar to those predicted using zonal winds, but the layer depths (Fig. 5) are thicker than those predicted by zonal winds because h_1 and h_2 are no

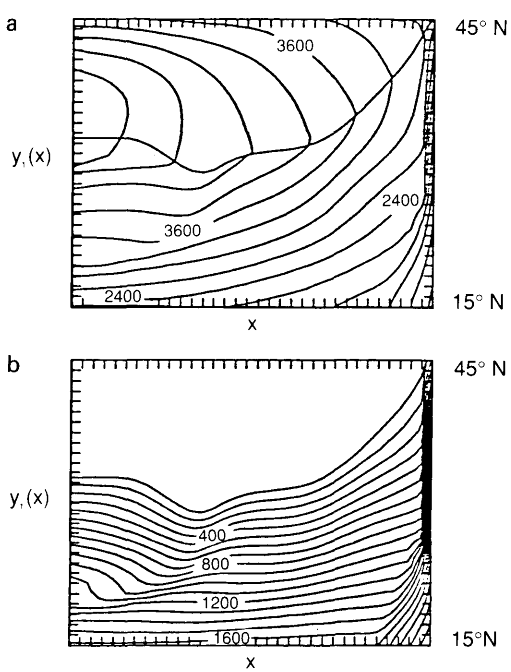

Fig. 5. As for Fig. 2, but using real wind data for the North Pacific spring (Hellerman, 1967, 1968). $c_0 =$ 3000 m. (a) The lower layer depth, h_2, (b) the upper layer depth, h_1.

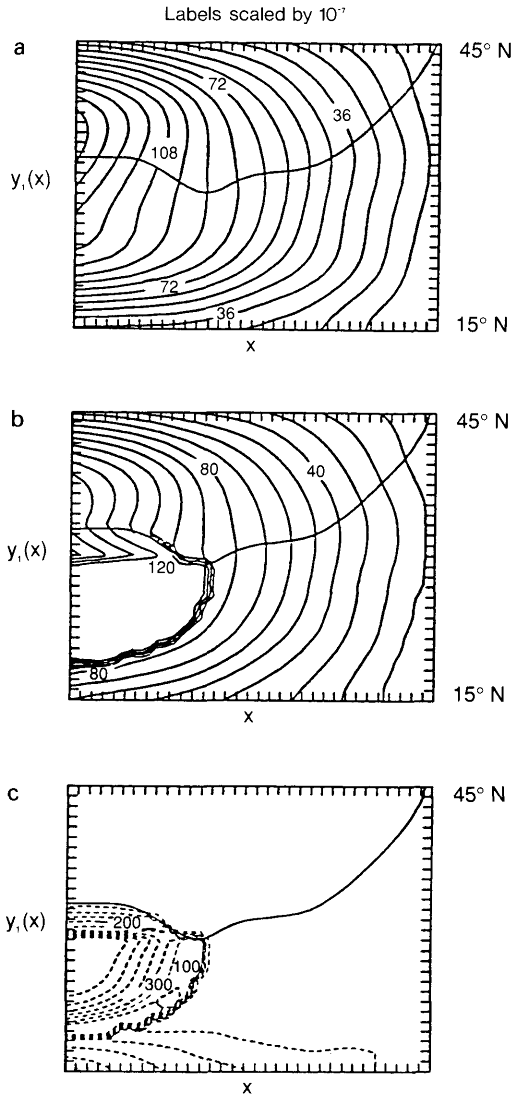

Fig. 6. As for Fig. 3, but using real wind data for the North Pacific spring (Hellerman, 1967, 1968). $c_0 =$ 3000 m. (a) The total streamfunction, Ψ; (b) the lower layer streamfunction, Ψ_2; (c) the upper layer streamfunction, Ψ_1.

longer required to be zero on the eastern boundary. The non-zonal outcrop shape also produces some interesting effects in the streamfunctions (Fig. 6), where the flow in the lower layer turns sharply east-west near the southernmost point of the outcrop. The upper layer flow is again weaker than the lower but shows more structure than that for zonal wind stress, in particular near the (open) western edge of the domain.

Figs. 7 and 8 show equivalent plots to Fig. 5 and 6 respectively for autumn in the North Pacific. The main features are similar, but since the outcrop shape is simpler (near zonal away from the coast) the results are closer to those observed for zonal wind stress. For this wind stress, the region in the south-east corner of the basin is not crossed by any characteristics emanating from the outcrop line. However, the flow here can be determined by tracing characteristics from the eastern boundary (where h_1 and h_2 are known). In the upper layer, some anti-cyclonic motion in this region results.

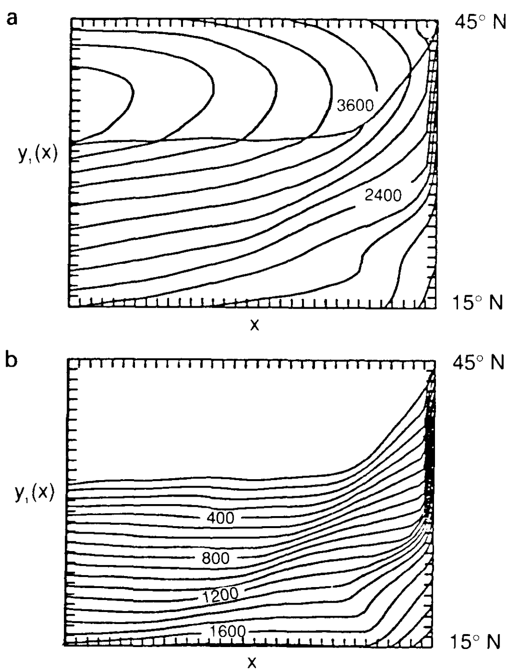

Fig. 7. As for Fig. 2, but using real wind data for the North Pacific autumn (Hellerman, 1967, 1968). $c_0 =$ 3000 m. (a) The lower layer depth, h_2; (b) the upper layer depth, h_1.

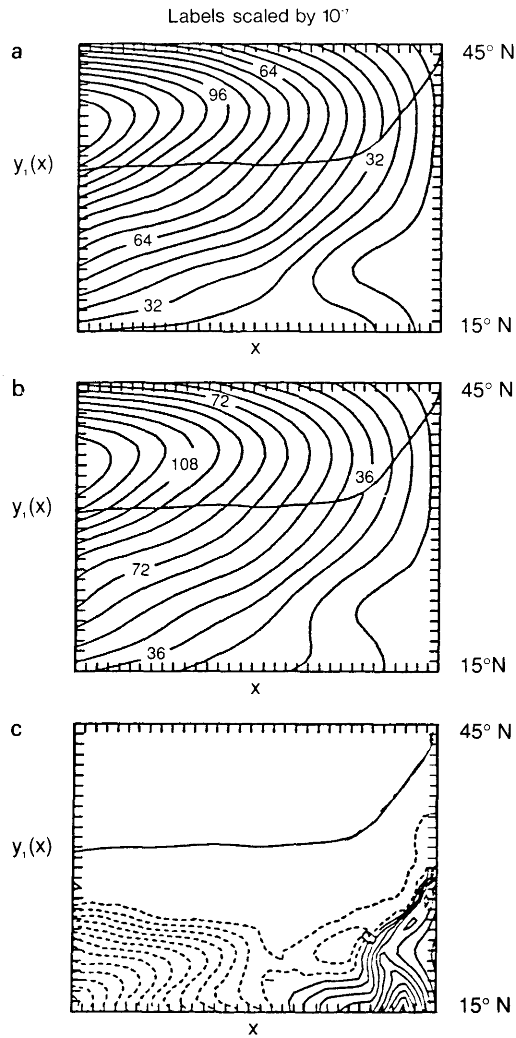

Fig. 8. As for Fig. 3, but using real wind data for the North Pacific autumn (Hellerman, 1967, 1968). $c_0 =$ 3000 m. (a) The total streamfunction, Ψ; (b) the lower layer streamfunction, Ψ_2; (c) the upper layer streamfunction, Ψ_1.

7. Interfacial friction

Consider the form of the momentum equations (1) and (2), with non-zero k_1, as $h_1 \to 0$. It is evident that the friction and wind stress terms must balance in the limit as $h_1 \to 0$, so that

$$\left.\begin{aligned} k_1(u_1 - u_2) &= \tau_0^{\,x}, \\ k_1(v_1 - v_2) &= \tau_0^{\,y} \end{aligned}\right\} \quad \text{when} \quad h_1 = 0. \tag{29}$$

Hence the outcrop is given, from (25), by

$$\mathrm{d}y_1/\mathrm{d}x = (\tau_0{}^y + k_1 v_2)/(\tau_0{}^x + k_1 u_2). \qquad (30)$$

Note the important result that as $k_1 \to 0$ this does not reduce to the outcrop equation for the frictionless model, (27). This is a consequence of the assumption that friction acts as a drag proportional to velocity, rather than transport. As a result the friction terms dominate the flow near the outcrop (where h_1 is zero), even though k_1 is small, and an entirely different dynamical balance is obtained to that when $k_1 = 0$ (where it was required only that the Ekman flux be along the surfacing line).

It is now possible to eliminate u_2 and v_2 so that the outcrop equation can be written solely in terms of the applied wind stress. Using (29), eqs. (3) and (4) give:

$$\left.\begin{aligned} v_2 &= k_1[(b_2/f)(h_1+h_2)_x - \tau_0{}^x/fh_2], \\ u_2 &= k_1[-(b_2/f)(h_1+h_2)_y + \tau_0{}^y/fh_2] \end{aligned}\right\} \quad \text{when } h_1 = 0. \qquad (31)$$

The lower layer depth, h_2, is known on the outcrop, since (10) holds with $h_1 = 0$, so that

$$h_2 = [(K+F)/b_2]^{1/2}, \qquad (h_1 = 0), \qquad (32)$$

where K and F are known in terms of the applied wind stress (eqs. (11) and (13)) and the lower layer depth, h_0, at one point on the eastern boundary (so that F_0 is determined by (15)). In addition, the Sverdrup relation (9) on the outcrop gives

$$(h_1+h_2)_x = K_x/2\{b_2(K+F)\}^{1/2}, \qquad (h_1 = 0), \qquad (33)$$

where use has been made of (32) and the definition of K. Finally, differentiating (10) with respect to y gives, on the outcrop,

$$(h_1+h_2)_y = (K+F)_y/2\{b_2(K+F)\}^{1/2}, \qquad (h_1 = 0), \qquad (34)$$

where use has again been made of (32). Now, substituting (32), (33) and (34) in (31) gives u_2 and v_2 on the outcrop solely in terms of prescribed quantities (τ_0 and h_0). The lower layer velocities may therefore be eliminated from (30), resulting in the outcrop equation:

$$\mathrm{d}y_1/\mathrm{d}x = \frac{\tau_0{}^y + (k_1/2)(K_x - 2\tau_0{}^x)\{(K+F)/b_2\}^{-1/2}}{\tau_0{}^x - (k_1/2)(K_y + F_y + 2\tau_0{}^y)\{(K+F)/b_2\}^{-1/2}}. \qquad (35)$$

Fig. 9 shows some possible outcrops given by equation (35). Figs. 9(a, b, c) are for data corresponding to spring in the North Pacific

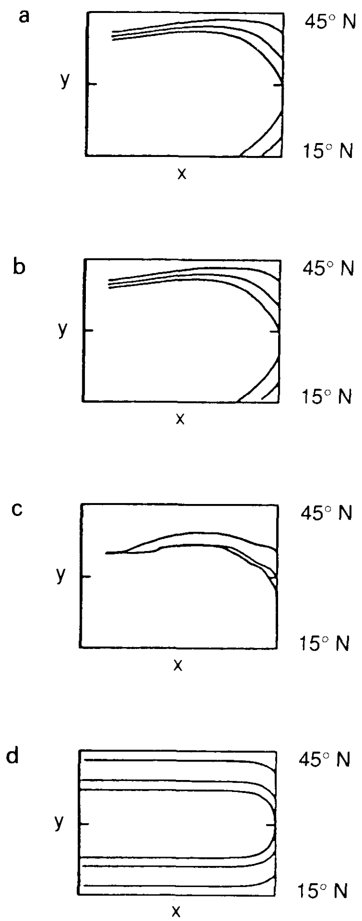

Fig. 9. Outcropping lines for the model with interfacial friction (parameter k_1). (a) $k_1 = 0$, real wind data (North Pacific spring); (b) as for (a) but $k_1 = 10^{-4}\,\mathrm{ms}^{-1}$; (c) as for (a) but $k_1 = 10^{-2}\,\mathrm{ms}^{-1}$; (d) as for (a) but analytical winds given by (36) with $\tau_0 = 0.1\,\mathrm{Nm}^{-2}/\rho_0$ and $L = 2000$ km.

(Hellerman 1967, 1968). There is no noticeable difference between Figs. 9a, b, calculated with $k_1 = 0$ and $k_1 = 10^{-4}$ m s^{-1} respectively, although an unrealistically large value of $k_1 = 10^{-2}$ m s^{-1} does change the outcrop shapes somewhat (Fig. 9c). It is reasonable, therefore, to approximate (35) by its form when $k_1 = 0$ (bearing in mind that this is not the same result obtained when friction is omitted from the model altogether). Fig. 9d shows outcrops for an idealized but non-zonal wind stress:

$$\tau^x = \tau_0 \sin(\pi y/\ell),$$
$$\tau^y = -\tau_0 e^{x/L}, \tag{36}$$

where L is the decay scale of the y-component of the wind stress away from the eastern boundary. The wind stress of (36) is an attempt to model the southward wind stress component near the west coast of North America. The outcropping lines with this wind stress give a reasonable approximation to those calculated with real data, whereas a zonal wind stress ($\tau^y = 0$) would give outcrops that are zonal (assuming the $O(k_1)$ terms in (35) are negligible).

Solutions for the individual layer depths and transport are not presented for the frictional model. The partial differential equation for h_1, (18), is no longer valid and eliminating the velocities from the equations of motion to obtain a single differential equation for the upper layer depth involves some tedious algebra. It also becomes apparent that such a differential equation would be elliptic and thus require specified boundary conditions on a closed curve, not readily provided in the domain under consideration. Another difficulty lies in the determination of the lower layer streamfunction, since potential vorticity is no longer conserved once this layer is subducted. The potential vorticity equation for the frictional model (derived by the same method as (23)) is now:

$$h_2 v_2 (f/h_2)_y + h_2 u_2 (f/h_2)_x = k_1\{[(v_1 - v_2)/h_2]_x - [(u_1 - u_2)/h_2]_y\} \tag{37}$$

(see Huang, 1987), so that lines of constant $q = f/h_2$ are no longer streamlines, although they may be nearly so if k_1 is small. In general, the frictional three-layer model does not allow such simple methods of solution as the frictionless model, and may be better approached by the numerical methods of Huang (1987).

8. Discussion

A three-layer, wind-driven model of ocean circulation has been developed and used to study outcropping in the subtropical gyre. It has been shown that the outcrop shapes can be determined in terms of the applied wind stress field and depend crucially on the presence of interfacial friction, the dynamical balance near the outcropping line being between the frictional and wind stress terms.

With zonal applied wind stress, it has been shown that only one outcrop intersecting the eastern boundary can exist in a frictionless model (a latitude circle at 30°N). Any number of constant latitude outcrops can exist for the more realistic model with interfacial friction, but in this case streamlines cannot be traced from the single layer region into the subducted lower layer. That is, including the terms which allow the crucial balance between friction and wind stress at the outcrop violates the conservation of potential vorticity in the lower layer, so the method of Luyten et al. (1983) cannot be used.

The effect of observed (seasonal data) wind stress forcing on the outcropping lines is also investigated. For the frictionless model the effect of non-zonal wind-forcing is to remove any possibility of zonal outcropping, at least near the coast, and outcrops must asymptote to the eastern boundary rather than intersecting it. For the more realistic frictional model, the outcrops are nearly zonal in the ocean interior but not so near the coast, where there is an important southward component of velocity. A simple analytical model of wind stress is suggested, with a southward component of wind decaying away from the eastern boundary, to give a better approximation to real wind data.

For the frictionless model, the individual layer depths and streamfunctions have also been calculated. Examples have been presented for both zonal wind stress and real wind data. The basic features are the same, with the upper layer deeper in the south of the basin and the gradient of the lower layer depth discontinuous at the outcrop. The upper layer flow is cyclonic and weaker than that in the lower layer (which does not, therefore, differ greatly from the total Sverdrup transport). It is important to note that a two-layer model, which assumes the lower layer is quiescent, does not therefore give a good approximtion to the flow. For observed wind data, the shape of the outcropping line affects the flow in the individual layers, producing a more complicated picture (with sudden changes in streamfunction direction) where the front is not zonal.

The major limitation of the three-layer model here is that it does not include a mixed layer or the effects of thermal forcing and cross-isopycnal flow on the outcropping lines. As pointed out by Huang and Bryan (1987), who present a numerical layered model with a mixed layer above, the effects of both wind and thermal forcing are important and an analytical model can only easily represent one or other extreme.

In addition, only a limited range of outcrops has been considered, in a restricted region. The effect of the western boundary current and also other possible outcropping lines (notably those with boundary layers) have been studied for two-layer models by Parsons (1969) and later authors (in particular Huang and Flierl, 1987, have considered the boundary layers in detail in a two-gyre basin). A three-layer model including all these effects has been studied numerically by Huang (1987).

9. Acknowledgments

HMW acknowledges a SERC research grant and the SERC travel grant that enabled her to visit the University of New South Wales during the course of this work.

REFERENCES

Hellerman, S. 1967. An updated estimate of the wind stress on the World Ocean. *Monthly Weather Review, 95*, 607–625.

Hellerman, S. 1968. (Correction to above). *Monthly Weather Review. 96*, 63–74.

Huang, R. X. 1987. A three-layer model for wind-driven circulation in a subtropical-subpolar basin. Parts I and II. *J. Phys. Oceanogr. 17*, 665–697.

Huang, R. X. and Flierl, G. R. 1987. Two-layer models for the thermocline and current structure in subtropical/subpolar gyres. *J. Phys. Oceanogr. 17*, 872–884.

Huang, R. X. and Bryan, K. 1987. A multilayer model of the thermohaline and wind-driven ocean circulation. *J. Phys. Oceanogr. 17*, 1909–1924.

Kamenkovich, V. M. and Reznik, G. M. 1972. A contribution to the theory of stationary wind-driven currents in a two-layer liquid. *Izv. Atmos. Oceanic Phys. 8*, 419–432.

Luyten, J. R., Pedlosky, J. and Stommel, H. 1983. The ventilated thermocline. *J. Phys. Oceanogr. 13*, 292–309.

Luyten, J. R. and Stommel, H. 1986. Gyres driven by combined wind and bouyancy flux. *J. Phys. Oceanogr. 16*, 1551–1560.

Niiler, P. P., Simco, E. and Larue, R. 1971. A two-layer model of the North Atlantic thermocline. *J. Phys. Oceanogr. 1*, 271–277.

Parsons, A. T. 1969. A two-layer model of gulf stream separation. *J. Fluid Mech. 39*, 511–528.

Pedlosky, J. 1986. The buoyancy and wind-driven ventilated thermocline. *J. Phys. Oceanogr. 16*, 1571–1582.

Pedlosky, J., Smith, W. and Luyten, J. R. 1984. On the dynamics of the coupled mixed layer-thermocline system and the determination of the oceanic surface density. *J. Phys. Oceanogr. 14*, 1159–1171.

Rhines, P. B. and Young, W. R. 1981. A theory of the wind-driven circulation, Part I: Mid-ocean gyres. *J. Mar. Res. 40 (Suppl.)*, 559–596.

Roden, G. I. 1975. On North Pacific temperature, salinity, sound velocity and density fronts and their relation to the wind and energy flux fields, *J. Phys. Oceanogr. 5*, 557–571.

Veronis, G. 1973. Model of the World Ocean circulation, Part I: Wind-driven, two-layer. *J. Mar. Res. 31*, 228–288.